Mechanical Characterization of Composites with Embedded Optical Fibers

JOSÉ M. A. SILVA,[1] TESSALENO C. DEVEZAS,[2,*]
ABÍLIO P. SILVA[2] AND JOSÉ A. M. FERREIRA[3]
[1]*Departmento de Ciências Aeroespaciais,* [2]*Departmento de Engenharia Electromecânica*
Universidade da Beira Interior, Calçada Fonte do Lameiro, 6201-001 Covilhã, Portugal
[3]*Departmento de Engenharia Mecânica, Universidade de Coimbra*
Pinhal de Marrocos, 3030 Coimbra, Portugal

(Received March, 2003)
(Accepted October 13, 2004)

ABSTRACT: The purpose of this investigation is to evaluate quantitatively and comparatively the effect of embedding optical fibers (OF) on the mechanical behavior of a carbon fiber-epoxy composite in order to verify whether their presence can possibly degrade the mechanical performance of the host material. The existing literature on this subject is not conclusive about the nature and intensity of this effect. Adding more reliable data to our systematic study contributes to this discussion favoring the conclusion about a harmful influence as a consequence of optical fiber embedment.

Three kinds of mechanical tests have been performed in this work: impact tests, static flexural tests, and fatigue tests. The results of some experiments point to a possible detrimental influence related to the presence of the OF, being it different in nature and intensity for each of these tests. The mechanical behavior in static loading conditions seems to be not significantly affected as a consequence of the presence of the OF, while that in impact and fatigue tests are strongly affected, even though this influence being physically distinct from each other. Based on these results, some discussion is made about the possible failure mechanisms that can explain the detected differences.

KEY WORDS: smart materials, fatigue, impact, laminated composites

INTRODUCTION

THE BROAD CONCEPT of smart structures is a modern scientific field that flourished some twenty years ago and yet is a subject of very intensive research. Intelligent material systems will have a great impact on numerous and varied applications [1] that will radically transform the basic concepts of engineering design in this century, mainly in the areas of robotic, architecture, civil engineering, aircraft, and space structures.

*Author to whom correspondence should be addressed. E-mail: tessalen@demnet.ubi.pt

0021-9983/05/14 1261–21 $10.00/0 DOI: 10.1177/0021998305050423

Basically, the anatomy of an intelligent material system is formed by actuators that behave like muscles, sensors that have the architecture and processing features of nerves, and the motor control system relying on communication and computational networks that mimics biological systems brains. Acting together, these systems can perform defined functions in response to external environmental changes, detected by suitable sensorial devices located within the structure [2,3]. Sensing may be considered then a prior function inherent to all intelligent material systems and structures.

Damage control, vibration damping, acoustic attenuation, health monitoring, and intelligent processing all require accurate information provided by sensors describing the state of the material system or structure. Sensing capabilities can be given by attaching sensors on the surface of the structure or by incorporating them within the bulk material forming the structure. The former is a common-use technology, while the latter constitutes a recent technological achievement and the theme of the present work.

Optical fibers (OF) embedded in a smart material can provide data in a couple of ways. First, they can simply provide a steady light signal (a laser beam for instance); interruption in the light beam indicates a structural damage that has snapped the OF. The second and subtler approach involves looking at key characteristics of the light: intensity, phase, or polarization. There has been considerable interest in exploiting these characteristics, with more than sixty different types of sensors being developed over the past decade [4]. Interferometric, refractometric, blackbody, modal domain, and time domain sensors were investigated for use in real-time damage assessment and in-service structural health monitoring.

One excellent example of a currently used smart material in the aerospace domain is composite materials, especially high-performance CFRP laminates, with embedded optical fibers. In addition to their extraordinary technological simplicity, these structures have great advantages resulting from the individual contribution and perfect symbiosis between composites and optical fibers [5,6]. The easiness of the optical sensor positioning procedure inside the host structure is one of the most notorious benefits when considering the material processing, commonly autoclave curing.

SETTING THE PROBLEM

Notwithstanding all the referred advantages, the embedment of fiber optic sensors and leads in any kind of material raises the critical issue whether embedded OF can possibly degrade the mechanical performance of the host material. In fact, it is important to note that the OF presence inside the material settles a defect that cannot be neglected, yet its physical dimension may increase by one order of magnitude than that of the carbon fibers belonging to the composite laminates [7]. The typical diameter of a single OF with coating can reach 200–250 μm, while the diameter of a carbon fiber does not exceed 7–8 μm. Thus an embedded OF may act like an elastic inclusion within the material, being a stress concentration agent whose disturbing effect is related to its size and positioning inside the structure [6].

This discrepancy in dimensions raises serious concerns regarding the manner of embedding OF and minimizing the local 'obtrusivity' [8] caused by its presence, that can be seen as a local flaw disturbing the natural plying sequence of carbon fibers.

Some recent investigations [6,8–10] concluded that the geometrical orientation of the OF relative to the adjacent laminate plies is a pertinent factor concerning its influence

on the material global mechanical performance. For instance, when the OF is embedded perpendicularly to the adjacent carbon fibers in unidirectional laminate plies, it produces a surrounding lenticular region rich in resin and without reinforcing fibers. This lenticular region acts like an interlaminar discontinuity that can be a potential source of damage in the presence of both static and dynamic loads.

In order to characterize this disturbing effect, some investigations were carried out during the last decade, evaluating possible degradations on the mechanical properties of different laminate configurations. Some of these results are summarized here.

Measures [5,11] investigated the performance of Kevlar-epoxy laminates with embedded optical fibers placed at different positions and under a tensile compression loading. The first results revealed a slight increase of the failure stress for some specimens, showing no major contribution of the optical fiber in any kind of damage caused in the structure. Also, Carman and Sendeckyj [9] obtained similar conclusions, mainly when the OF was placed parallel to the reinforcing fibers.

Roberts and Davidson [12] tested several carbon-epoxy specimens subjected to tension, compression, and interlaminar shear loading, finding a considerable influence resulting from the presence of the OF. These authors detected an average decrease in the strength of the material (about 26%) for the case of perpendicular embedment under compressive loads. On the other hand, no noticeable prejudice on the material behavior could be observed as effect of the dimension and coating nature of the optical fiber; for diameters $< 160\,\mu m$ and for polyamide coatings.

In the context of static loading, Correia and Devezas [13] carried out experimental bending tests involving carbon-epoxy laminates with embedded OF that confirmed some minor influence on the material's overall mechanical properties when the OF was perpendicularly aligned. Their results showed a slight decrease of strength and stiffness, 9 and 11%, respectively.

In the particular situation of positioning the OF within a 0/45° interface, the sensor perturbation seems to be notorious, such as the one concluded by Surgeon and Wevers [14] through flexural tests that resulted in more than 50% loss of strength in some cases.

Considering the dynamic loading scenario, we can find some interesting results in the literature. In a previous publication, the present authors related about the strength reduction in fatigue tests for some configurations of OF embedded in CFRP composites [15]. Sirkis and Dasgupta [8] gathered general information from several studies concerning fatigue behavior during the late 80s, allowing to infer about the minor influence of the OF when embedded parallel to the reinforcing fibers, as also determined by Jensen and Koharchik [16] in tensile fatigue tests using thermoset composites. Yet when the OF is embedded perpendicular to the adjacent plies, we can find references to some degree of damage in the sensor's neighborhood caused by low frequency tensile fatigue tests. This fact is corroborated by Jensen and Brzenchek [17], whose investigations using cross-ply graphite-bismaleimide laminates under tensile fatigue tests revealed a substantial strength reduction (about 25%) for specimens with OF oriented perpendicular to the direction of the applied load and also to the adjacent reinforcing fibers.

Carman and Sendeckyj [9] referred to some properties degradation for composites submitted to compression fatigue tests with 250 μm diameter embedded OF, which could be detected since the first loading cycles. However, a more recent investigation [18] concluded that no degradation of the composite properties could be imputed to the presence of the OF for tension fatigue loads leading to low strains.

Also, Surgeon and Wevers [14] conducted an experimental investigation using carbon-epoxy laminates with different layup configurations and containing optical fibers with a diameter of 140 μm and a polyimide coating. The OF were embedded transversely to the load direction and in several positions considering the following adjacent laminate plies: 0/45°, 45/−45°, −45/90°, and 90/−90°. Their fatigue tests used a 5 Hz frequency, a stress ratio equal to 0.1, and three different applied stress levels. The results from all specimens subjected to the lowest stress level (50%) showed no sign of damage till the stipulated limit, while for the other two load levels it was possible to infer about a possible detrimental effect of the embedded OF. In fact, for the intermediate stress level (65%) and, in particular, for OF placed at 0/45° and −45/90° interfaces, a degradation of the material properties was noticed. Such degradation was evinced by premature specimen failures imputed to large local distortions in the vicinity of the OF and, in some cases, evident delaminations affecting those interfaces. The highest stress level (80%) led to premature failures for all configurations, but the large dispersion of the results was an impediment for more detailed conclusions.

Another important application of OF is that of impact damage detection via fiber breakage sensor [8], referred hereafter as on–off sensor, that started in the early 1980s. Looking at the published literature, we can infer that the majority of impact experiments performed on composite materials containing optical fibers has not been directed toward assessing the effect of embedded optical fibers on the impact response, but toward assessing the survivability of an OF in a composite subjected to impact loading. In fact we can find in the literature some information about the relationship between fiber treatment (chemical etching), depth and orientation in the layup, and the threshold impact energy for the effectiveness of OF as damage detection devices [5,19].

While almost all published reports did not specifically investigate the influence of embedded OF on damage progression in impact-loaded composites, there are some good investigations in this subject performed in the early 1990s by Chang [20] and Sirkis et al. [21]. In these studies, the effect of impact loading was examined for carbon/epoxy composites containing OF ranging in diameter from 100 to 600 μm, using three different stacking sequences (cross-plied, quasi-isotropic, and unidirectional). The authors concluded that small diameter optical fibers (100 μm) do not significantly influence the progression of damage. But in this research, the authors used only a single OF embedded at the laminate midplane subjected to very low impact energies applied to very thin laminates.

Considering the abovementioned investigations altogether, we can observe that these results fall short of being conclusive, and in some cases are even contradictory. This fact motivated the present work, which represents a compilation of extensive experimental investigation carried out at the University of Beira Interior concerning the overall mechanical properties characterization of carbon-epoxy laminates with embedded optical fibers, considering the cases of static, dynamic, and impact loading scenarios.

EXPERIMENTAL PROCEDURES

All samples produced for the impact experiments were manufactured from Ciba-Geigy Vicotex SXHR M18/32%/134/HTA prepregs, using 18 plies laid up symmetrically, resulting in plates with ≈2.5 mm thickness. Multimode optical fibers, Newport F-MLD 100 μm, were manually embedded into the specimens during sample layup. The specimens

were cured in an autoclave under a pressure of 7 bar for 2 h at 180°C. KA2HA Diatex polyimide film was used to protect points of ingress and egress. The integrity of all fibers was examined prior to impact testing by observing the continuity of a 632 nm light beam from a Helium/Neon laser powered at 10 mW.

The samples with dimensions of $60 \times 60\,mm^2$ were impacted at low velocities using a single drop-weight impactor of a Impactomat machine provided with a projectile of mass 2.7 kg, cylindrical in shape with a rounded 20-mm diameter nose. The plates were placed in fixtures that simulated fully clamped boundary conditions and were impacted once, at energies ranging from 5 up to 40 J, when penetration of the projectile could be observed fully.

The resulting impact damage on the specimens with and without OF was assessed in three ways: by ultrasonic C-scan imaging with a Ultrapac equipment, by visual observation of the impacted and back surfaces, and by optical microscopy observation of cross sections cut up from the central crushed (due to the impact) region. For the specimens with embedded OF, the survivability of the fibers was observed using the criterion of continuity of a laser beam.

Table 1 shows the nine stacking sequences used for the 18-ply layup specimens, with and without OF.

As can be seen, the OF were embedded in three different positions: 1 – in the middle of the ply; 2 – between the third and fourth laminates referred hereafter as near the impact surface (nis); and 3 – between the 15th and 16th laminates, referred hereafter as opposite to the impact surface (ois). For the configuration type A (unidirectional carbon fibers), two arrangements of the OF were used: parallel to the structural fibers (A1) and perpendicular to the structural fibers (A2, A3, and A4). In the configuration type B (cross-ply arrangements), the OF were placed always parallel to the structural ones. The configurations type B3 and B4 are shown in Figure 1.

Considering now the static and fatigue tests, the specimens were manufactured using a Seal Texipreg HS 110 REC prepreg composed by unidirectional high strength carbon fibers and an epoxy matrix with a volume fraction of 32%. Autoclave curing with temperature and pressure values of, respectively, 125°C and 7 atm was the process used to obtain the best material properties and its lowest dispersion when considering different specimen sets. Each specimen had a rectangular shape ($150 \times 25\,mm^2$) and a nominal 2 mm thickness resulting from a total of 18 plies stacked in different sequences (with or without an embedded OF), resulting in the configurations presented in Table 2.

Table 1. Notation and types of specimens used in impact tests.

Type	Stacking sequence	Optical fiber
A0	$[0^\circ]_{18}$	No
A1	$[0_9/\text{OF}\ (0^\circ)/0_9]$	Yes
A2	$[0_9/\text{OF}\ (90^\circ)/0_9]$	Yes
A3	$[0_3/\text{OF}\ (90^\circ)/0_{15}]$	Yes
A4	$[0_{15}/\text{OF}\ (90^\circ)/0_3]$	Yes
B1	$[0_2/90_2/0_2/90_2/0]_S$	No
B2	$[0_2/90_2/0_2/90_2/0/\text{OF}\ (0^\circ)/0/90_2/0_2/90_2/0_2]$	Yes
B3	$[0_2/90/\text{OF}\ (90^\circ)/90/0_2/90_2/0_2/90_2/0_2/90_2/0_2]$	Yes
B4	$[0_2/90_2/0_2/90_2/0_2/90_2/0_2/90/\text{OF}\ (90^\circ)/90/0_2]$	Yes

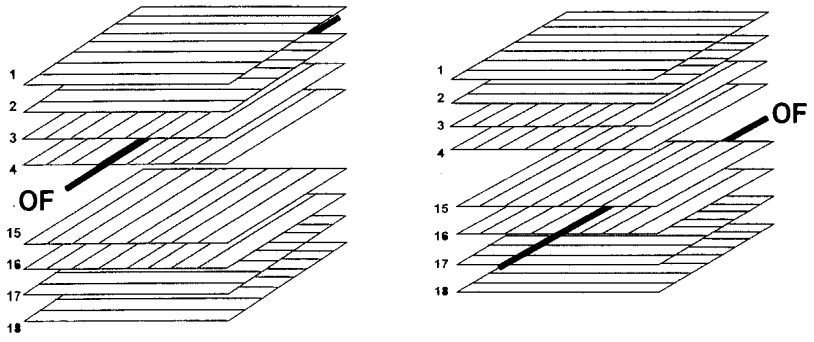

Figure 1. *Cross-ply layup of carbon fibers using 18 laminates with OF placed (a) between the third and fourth laminates (near the impact surface – nis), and (b) between the 15th and 16th laminates (opposite to the impact surface – ois).*

Table 2. Notation and types of specimens used in static and fatigue tests.

Type	Stacking sequence	Optical fiber
A	$[0^\circ]_{18}$	No
B	$[0_2/90_2/0_2/90_2/0]_S$	No
C	$[90_2/0_2/90_2/0_2/90]_S$	No
A-T	$[0_3/OF/0_{15}]$	Yes
A-M	$[0_9/OF/0_9]$	Yes
B-T	$[0_2/90/OF/90/0_2/90_2/0_2/90_2/0_2/90_2/0_2]$	Yes
B-M	$[0_2/90_2/0_2/90_2/0/OF/0/90_2/0_2/90_2/0_2]$	Yes

For the three-point bending fatigue tests performed in this work, the D790 ASTM standard was used in order to prevent possible collateral effects related with different loading modes, such as interlaminar shear.

All specimens were carefully characterized before the fatigue tests with the objective of determining an average value for the ultimate strength of each specimen configuration. Being so, static three-point flexural tests were performed, accordingly with the referred standard, using a Zwick 1435 universal mechanical testing device equipped with a 5-kN load cell.

Fatigue tests were conducted on an Instron 1341 universal hydraulic testing system, with a 25 kN installed load cell, coupled to a FastTrack 8800 digital controller for data acquisition and monitoring of all test parameters.

Finally, in order to more adequately qualify and quantify the damage present in the structure, some acoustic emission tests were performed using a Marandy MR1004 equipment coupled with a broad range piezoelectric transducer, which was connected to an appropriate software in order to acquire the total countdown of all events detected above a preset reference threshold voltage.

Microstructural observations were also effectuated using both a Hitachi S-2700 scanning electron microscope and a Leica MEF4M metallographic microscope.

RESULTS AND DISCUSSION

Impact Tests

Starting with impact tests, and considering unidirectional composites (configuration type A), no difference in behavior could be detected between specimens with and without OF, since all specimens fractured throughout for the lowest impact loading energy (5 J) allowed by the impact testing fixture used. However, for the cross-ply arrangements (configuration type B), some different behavior could be observed. The most interesting difference in behavior regards the survivability of the OF for the configuration B3 (nis) as compared with the configuration B4 (ois) that is presented in Figure 2.

When placed between the third and fourth laminates, the OF can act well (it works) as an on–off sensor, since it always breaks for energies larger than 10 J, what does not happen for energies lower than 9 J, with some uncertainty in the 9–10 J range (in this energy range, it was observed that sometimes the OF breaks, sometimes not). However, when placed between the 15th and 16th laminates (hence opposed to the impacted surface), the function of the OF as an on–off sensor seems to be not possible. No breakage of the OF is observed all over the range from 5 to 17.5 J, with the exception of the 9–10 J interval, where the same uncertain behavior of the configuration B3 was observed. This means sometimes the OF breaks, sometimes not. This observation sounds as an apparently 'unrealistic' finding, and it is difficult to explain. The meaning of the continuous curves in Figure 2 (crack length) is explained later, together with some speculation on the cause of this curious phenomenon.

The numerical value of the minimal impact loading energy to cause the breakage of the OF is probably a function of the thickness of the specimen. Since the thickness of the used specimens was roughly constant of the order of 2.5 mm, the present results point to a minimal specific energy of about 4×10^3 J/m when embedding the OF near the impact surface, corresponding to the threshold value of 10 J found in these measurements.

The impact-induced delaminations in 18-ply carbon/epoxy composites with 100 μm multimode optical fibers placed at the two different positions, shown in Figure 1 were also investigated. The first question that arose was how to evaluate the impact damage (delamination), if using for instance X-ray or ultrasonic c-scan nondestructive evaluation

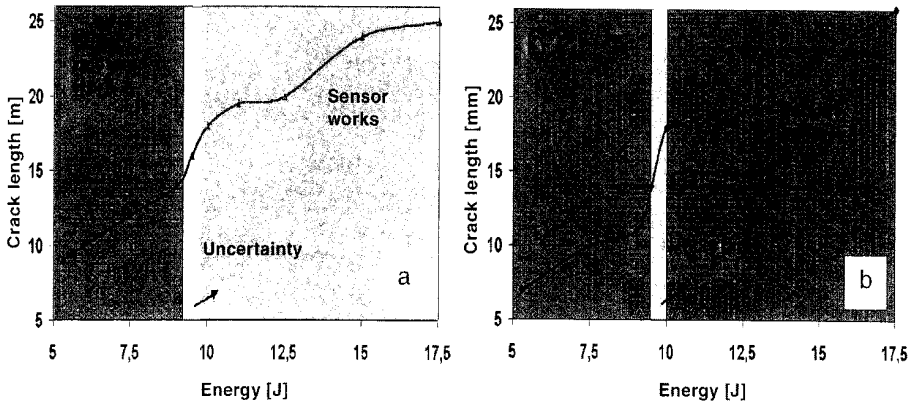

Figure 2. *Different impact behaviors of 18-ply carbon/epoxy composites with embedded optical fibers, (a) configuration B3, optical fiber placed near the impact surface (nis), and (b) configuration B4, optical fiber opposed to the impact surface (ois).*

techniques or destructively using a sectioning procedure. It was decided to use the ultrasonic c-scan technique and microscopic observations of cross sections of the through-the-thickness direction, but another procedure was added, as explained hereunder. The most important observations are listed here.

(i) The most visible effect of impact loading on the tested specimens is the appearance of a crack in the middle of the surface opposed to the impacted one; this crack consists of a fiber/matrix splitting of the external 0_2° ply and could be clearly observed even before any visible effect (development of a dent) appeared on the impacted surface;
(ii) The cracking or splitting phenomenon is proportional to the impact loading energy, that is, it increases steadily with increasing impact energy;
(iii) The cracking effect is more severe in specimens with embedded OF than for specimens without OF for the same impact loading energy.

In the face of these observations, it was decided to measure the length of the crack induced in the surface opposed to the impact as an impact damage characterization parameter. Figure 3 shows the results obtained for specimens with cross-ply arrangements, with and without OF.

The graphs in Figure 3 show clearly the difference in behavior between specimens without OF and specimens with OF. For the former, there is a threshold impact energy of approximately 7 J; below which no visible crack is observable on the surface opposed to the impacted one. In specimens with OF, the cracking occurs even for the minimal impact energy (5 J) and for higher energies, specimens with OF have always a crack length larger than specimens without it. However, the most important observation is the fact that the crack length for the configuration B3 (nis) is almost always larger than that for the configuration B4. The continuous curves shown in Figure 2 are the same pictured in Figure 3, respectively for the B3 (Figure 2a) and B4 (Figure 2b) configurations.

Optical microscopy observations of through-the-thickness cross sections of the impacted zone for specimens with and without OF allowed to come to another series of

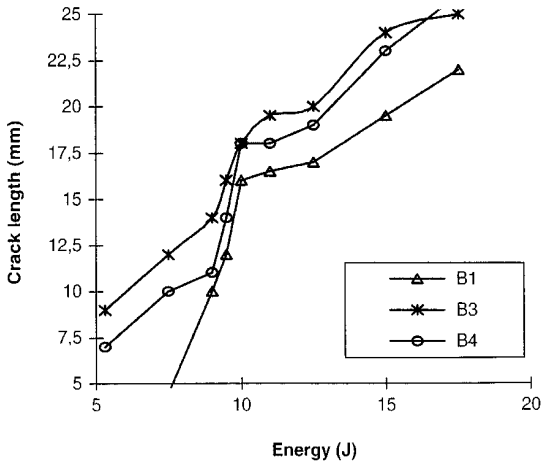

Figure 3. *Results of the impact tests (crack length) obtained for specimens with cross-ply arrangements. (B1): without OF, (B3): OF placed between the third and fourth laminates, (B4): OF placed between 15th and 16th laminates.*

conclusions that can contribute for the interpretation of the observed phenomena. These are:

(i) The impact damage consists of delaminations, which are more extensive toward the back face, and have a top-down aspect as a cascade process;
(ii) These delaminations always occur between layers with different carbon fiber orientation (for instance between 0_2° and 90_2° or vice versa) and seems to be a simple loss of adhesion between these layers;
(iii) This progressive delamination seems to radiate from the point of impact in the through-the-thickness direction, being connected by inter-lamina and shear cracks;
(iv) The damage in the last lamina, already described as the cracking/splitting of the fiber/matrix structure, is mainly caused by a dramatic impact-induced flexural deformation;
(v) Finally, for low energy impacts in specimens with OF, it was possible to recognize that the delamination phenomenon starts in the interface immediately below the optical fiber.

Figure 4 illustrates points (i)–(iii) and Figure 5 illustrates point (iv), while in Figure 6, a SEM image reveals the delamination described in point (v) occurring immediately below the optical fiber in a specimen with stacking sequence B4.

The observation of the cascade-fashioned propagation of delaminations in the through-the-thickness direction is in perfect agreement with the experimental results already presented by Poon et al. [22] when investigating impact damage in toughened carbon/epoxy composites. The present investigation points to the observation of the same phenomenon, but clearly enhanced by the presence of embedded optical fibers, which leads to the conclusion that their introduction in the composite structure significantly influences the impact behavior of the host material.

The impact loading generates a stress wave that propagates from the point of impact toward the back face, being reflected at the lowest ply. The observed delamination results from the fact that the embedded OF acts as an inclusion that induces a local strain

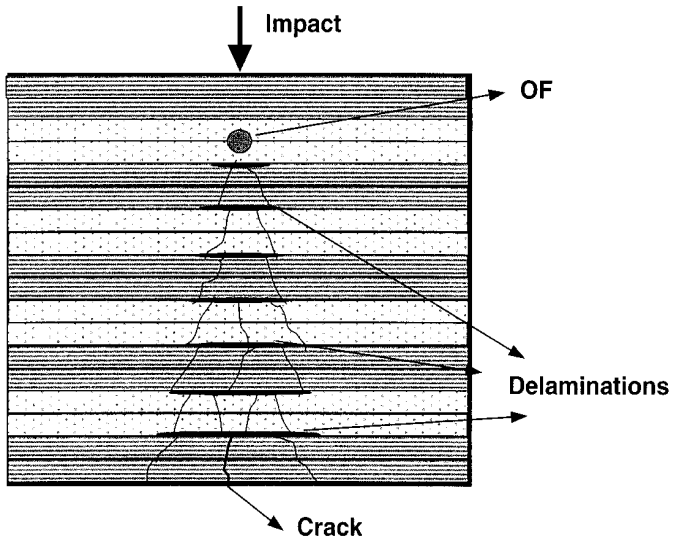

Figure 4. *Impact damage propagating in the through-the-thickness direction in a cascade fashion.*

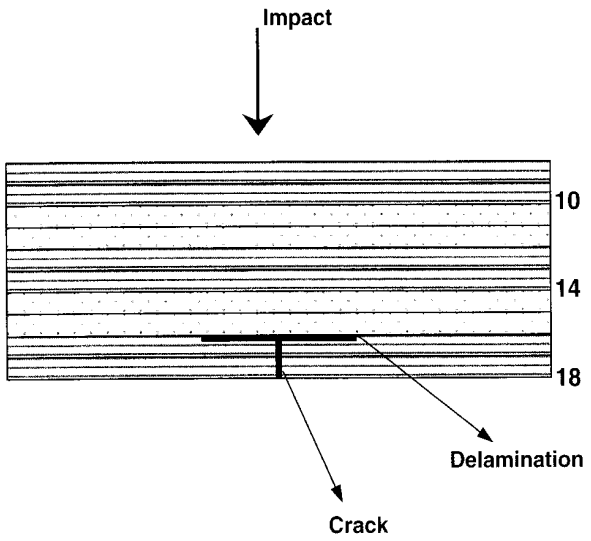

Figure 5. *Damage in the last lamina caused by impact-induced flexural deformation.*

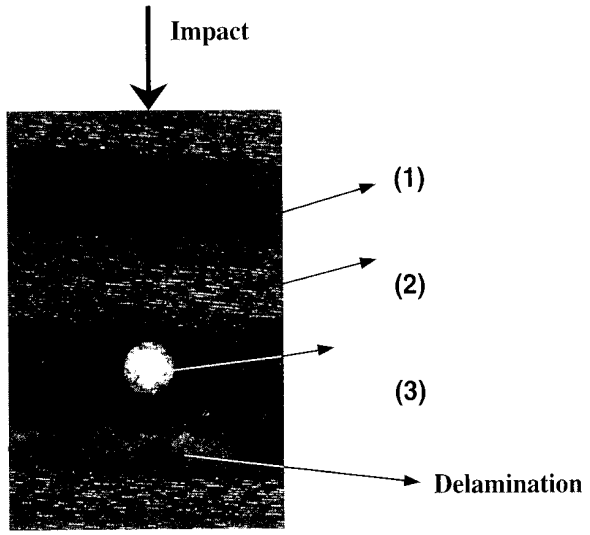

Figure 6. *Scanning electron micrograph image of a delamination damage for low energy impact occurring in the interface immediately below the optical fiber in a specimen with stacking sequence B4. Magnification 50×. (1) 11th and 12th layers parallel to the OF; (2) 13th and 14th layers perpendicular to the OF; (3) optical fiber embedded between 15th and 16th layers parallel to the carbon fibers.*

concentration that interacts with the stress wave induced by the impact loading. This interaction of the stress wave with the local strain field surrounding the OF results in an energy release, that intensifies the amplitude of the stress wave and, consequently, enhances the impact damage. The singular behavior pointed out in Figure 2 in the 9–10 J region of impact energy may be due to some kind of resonance effect between the stress wave and the geometry of the specimen, and seems to be independent of the position of the OF. This curious behavior was detected through measurements of 5 specimens for each

energy level chosen (9.5, 10, 11, 12.5, and 15 J). It was observed that for the 9–10 J energy level and for the configuration B4, the OF broke in some cases (≈50%), which could not be observed for the higher energy levels. Eight more specimens were then tested in this energy range (9–10 J, configuration B4), with the same statistical results. These results claim for a more extensive research for a comprehensive explanation.

Static Tests

In the flexural tests, the values for the elastic modulus (E_1) and maximum strength resistance (σ_r) were determined by the control system software using, respectively, the following equations:

$$E_1 = \frac{3PS}{2wt^2\varepsilon} \tag{1}$$

$$\sigma_r = \frac{3PS}{2wt^2} \tag{2}$$

where, P is the applied load, S is the distance between supports, w and t are, respectively, the specimen width and thickness and, finally, ε is the strain obtained from the control software of the test system.

Three to five tests, at similar conditions, were performed considering each specimen configuration. Table 3 presents the elastic modulus and flexural strength mean values obtained for each configuration (compare with Table 2).

From these results, it is possible to conclude that, as expected, unidirectional type configurations with or without embedded OF (A, A-M, and A-T) have the highest values for stiffness and strength when compared with cross-plied configurations, while on the other extreme, cross-ply type C laminates show the worst values for these properties. Thus, and in order to comply with the ASTM standard's recommendations [23], this configuration was rejected from further tests since it implied a very large deflection of the specimens, causing both undesirable shear stress loadings in the laminate's middle plane and severe work conditions at the test machine's actuator for the pretended load frequency (almost corresponding to its limit situation). So, only type A and B specimens' configurations, with or without OF, were considered for fatigue tests.

Table 3. Elastic modulus and flexural strength resistance for each configuration of specimens.

Specimen type	E_1 (GPa)	Standard deviation (E_1)	σ_r (MPa)	Standard deviation (σ_r)
A	96.9	10.8	1340.5	115.7
B	71.9	2.8	1045.9	7.5
C	39.6	1.22	898.8	12.7
A-T	94.8	7.41	1259	26.5
A-M	99	1.73	1384	35.5
B-T	71.4	2.55	1019.7	22.7
B-M	73.2	4.53	1107.5	29.6

Table 4. Stiffness and strength variation between analogous configurations with or without OF.

Type of specimens	ΔE_1 (%)	$\Delta\sigma_r$
A A-T	− 2.16	−6.08
A A-M	+ 2.17	+3.2
B B-T	− 0.69	−2.5
B B-M	+ 1.81	+5.9

The results listed in Table 3 confirm the previous conclusion of other investigators about a very small influence of the OF on the static mechanical properties of the host material. Only a slight decrease in the stiffness and strength values was detected in the case of sensor embedment between the third and fourth plies of unidirectional laminates (A-T configuration). Type B specimens revealed a similar practically indifferent behavior regarding the OF presence, having even shown a small increment of these properties for the B-M configuration, i.e., with embedded OF in the laminate middle plane.

Table 4 allows to compare the stiffness and strength variation between analogous configurations with and without OF embedment.

Fatigue Tests

Fatigue tests were carried out using a sinusoidal loading type for two maximum stress levels, concretely 75 and 90% of the ultimate strength value determined in the static tests. It was decided to use a 6 Hz frequency, in order to prevent possible thermal effects that could degrade the material behavior, and a 0.1 stress ratio. Time constraints imposed a total number of 500,000 load cycles as the stipulated test limit.

All fatigue tests turned to type A and B specimens (without OF) and A-T, B-T, A-M and B-M (with embedded OF between the third and fourth or ninth and tenth plies). A comparative study was intended to be carried out on a possible baneful effect related to the OF presence in the material considering three test variables: the laminates stacking sequence, the OF position in relation to the specimen's thickness, and the applied load level.

In general, almost all configurations revealed only a subtle stiffness decrease for the lower applied stress level (75%). However, the higher stress level (90%) led to an evident elastic modulus decrease in some cases, specially in those configurations with embedded OF, as some premature material failures occurred for a small number of load cycles. Therefore, only the graphs regarding the stiffness decaying for higher stress levels (90%) are subsequently presented.

Starting with unidirectional laminates, Figure 7 presents the elastic modulus variation for specimen types A, A-T, and A-M. As shown, type A configuration experienced an average stiffness decrease of approximately 14% (this value was only about 8% for the lower 75% stress level). At the same time, and considering the highest stress ratio (90%), the premature failure of two A-T specimens and all A-M specimens was detected. In particular, the latter configuration revealed to be very critical, since all final failures occurred for a very low number of cycles (1953, 12,008, and 76,536 cycles). The same A-M

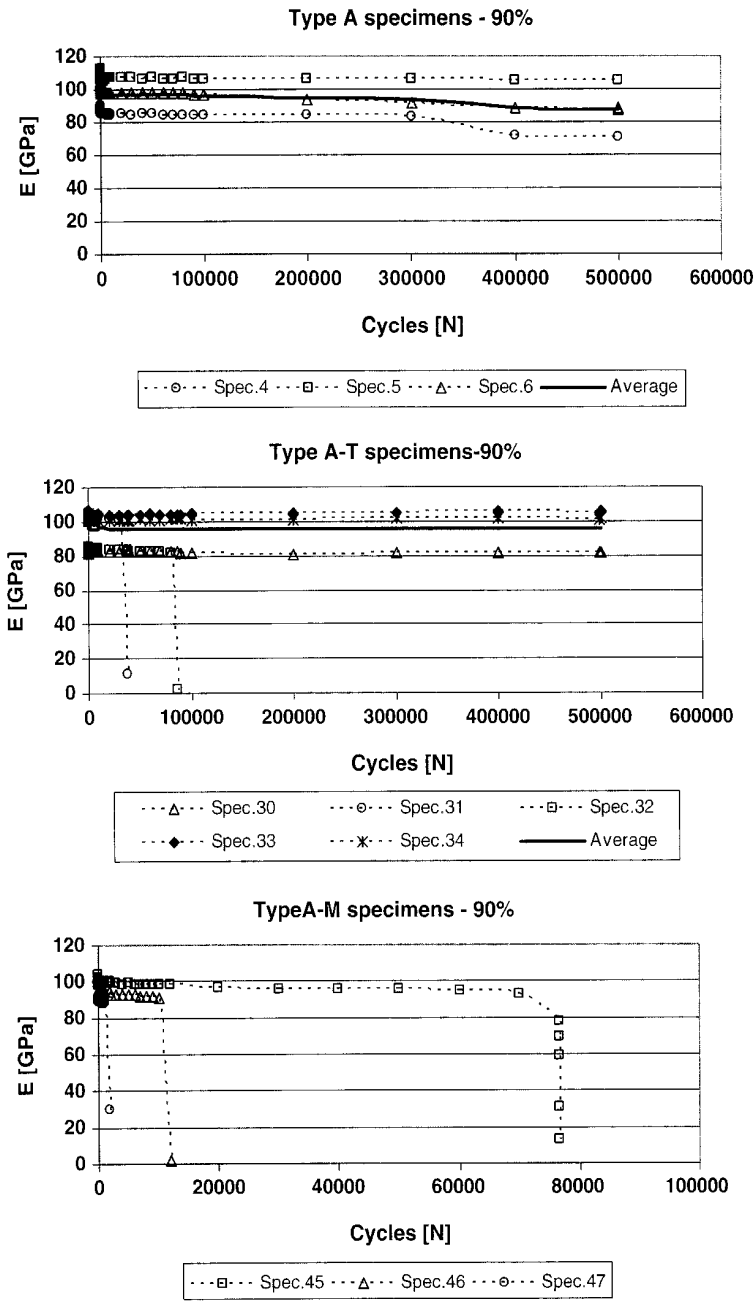

Figure 7. *Elastic modulus variation in fatigue tests for type A, A-T, and A-M specimens.*

configuration, but considering the lower loading condition (75%), revealed a very subtle stiffness decaying of approximately 4%.

These results were in someway surprising, since it was expected that OF embedment between the third and fourth plies could be the worst case, due to the presence of the sensor in the most critical region of the laminate regarding direct stresses. It is also

important to notice that for this configuration (A-T), and considering apart the two fractured specimens, any degradation of the material properties for the remaining specimens (only 4 and 2%, respectively, for the 75 and 90% stress levels) was evident.

Cross-ply laminates generally revealed to have less fatigue resistance than unidirectional configurations. Type B specimens (without embedded OF) corroborate this fact, for from a total set of five specimens subjected to the higher stress level (90%), two suffered from a premature failure (at 13,791 and 55,597 cycles) and only one survived the whole fatigue test without showing any visible superficial damage. The other two specimens had a notorious superficial degradation evinced by the existence of delamination and cracking in the laminate region subjected to compression loads. Even for the lower stress level case (75%), this configuration revealed an average stiffness decrease of about 6%.

The embedment of the OF in cross-ply configurations causes a remarkable detrimental effect, mainly when the sensor was placed in the laminate middle plane (B-M specimens). In this case, all specimens failed for a very small number of cycles, namely, 1219, 1394, and 5833 cycles. For B-T configuration, an average stiffness decrease of approximately 12% was observed and only one specimen failed immediately after the beginning of the test.

Figure 8 shows the variation of the elastic modulus for all these types of cross-ply laminates along with the number of test cycles. It is interesting to note that B-T configuration should have been the most adverse, for in this case OF embedment was perpendicular to laminate adjacent layers and therefore, it provoked a lenticular resin-rich region in its neighborhood. However, the configuration B-M revealed to be the most critical, as we can conclude from the premature failures of all specimens shown in Figure 8. As explained above, when discussing Figure 7, this phenomenon (embedment in the middle plane as the worst case) was also observed for the unidirectional laminates, probably due to the fact that the middle plane is a highly critical region regarding the existence of shear stresses.

Table 5 summarizes the fatigue tests results for unidirectional and cross-plied laminates with embedded OF (types A-M, B-M, A-T, and B-T), and considers the two applied ratios between fatigue maximum stress and ultimate static strength ($k = 0.9$ and $k = 0.75$).

In order to characterize the damage evolution during cyclic loading and trying to qualify its nature, some acoustic emission (AE) tests were performed only for the highest stress level (90%) and for the configuration types A, A-M, A-T, and B. The piezoelectric transducer was placed at the same position for all specimens, and special attention was devoted to the gripping procedure in order to minimize undesirable environmental noise. Also an adequate threshold level was considered for each test in order to filter possible erroneous signals resulting from the hydraulic machine's normal operation. Figure 9 shows the experimental setup used for the acoustic emission tests schematically.

The AE tests were limited to a total of 20,000 cycles. These tests allowed concluding that regarding total countdowns, damage evolution was a linearly increasing phenomenon. Qualitatively, it is also possible to use these tests to distinguish among different damage mechanisms acting during cyclic loading. In this sense it was possible to detect distinct acoustic emission levels exhibiting a clearly nonlinear behavior and, therefore, to relate them with the intensity of damage.

Some investigators, like Surgeon and Wevers [24], have already established a good conformity between the emission's intensity and the type of damage occurring in composite laminates with embedded OF. Basically, low-level emissions can be attributed to weakening phenomena (like matrix cracking), while more intense damage (like delamination and fibers breakage) results in medium or high-level emissions. Our measurements

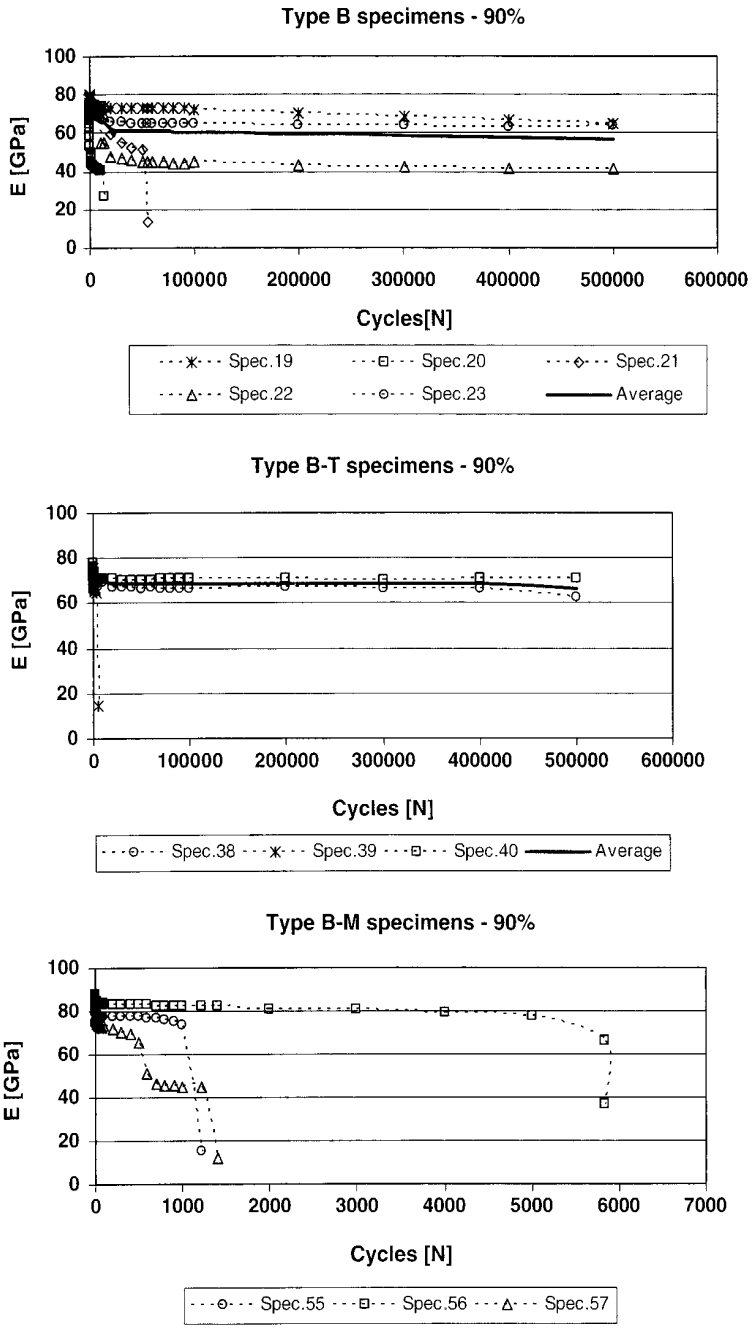

Figure 8. *Elastic modulus variation in fatigue tests for type B, B-T, and B-M specimens.*

allowed to identify the described damage evolution phenomenon, following a nonlinear tendency starting from low level occurrences, such as matrix cracking, and ending with high intensity catastrophic events, possibly strong delaminations or a large number of fiber breakage, just preceding the final material rupture. Figure 10 shows this behavior

Table 5. Compilation of the results for fatigue tests in laminates with embedded OF.

Configuration	K: ratio between fatigue maximum stress and ultimate static strength	
	$k = 0.9$	$k = 0.75$
A-M	Three specimens with premature failure (1953, 12,008, and 76,536 cycles)	Three specimens without significant damage after 500,000 cycles
B-M	Three specimens with premature failure (1219, 1394, and 5833 cycles)	Three specimens without significant damage after 500,000 cycles
A-T	Two specimens with premature failure (37,515 and 86,650 cycles) and three without significant damage after 500,000 cycles	Three specimens without significant damage after 500,000 cycles
B-T	One specimen with a premature failure (4518 cycles), one with strong delamination after 500,000 cycles and one without significant damage.	Three specimens without significant damage after 500,000 cycles

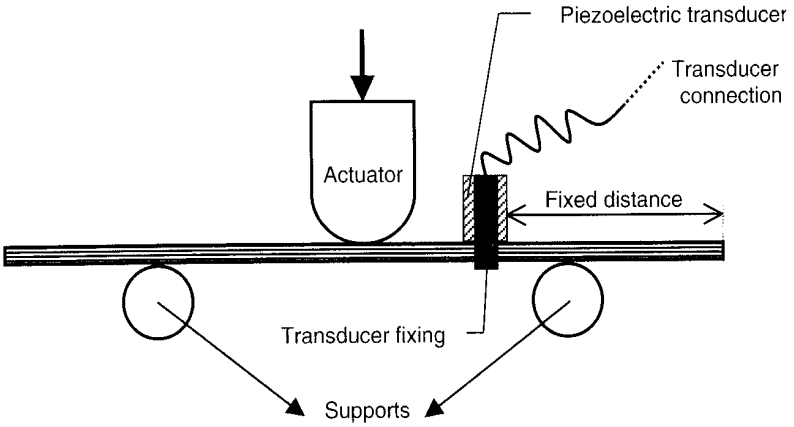

Figure 9. *Experimental setup for the acoustic emission measurements.*

for type A-M specimens, presenting both total countdowns and medium and high level acoustic emissions.

Optical and electronic microscopy observations constituted another relevant part of this investigation intending to assess the damage mechanisms existing in the surroundings of the OF, as well as a possible fatigue pattern at the fracture zone.

At the first stage, two specimen configurations were considered with different OF embedment orientation (parallel and perpendicular) in order to confirm the distortion related to the existence of a lenticular region. As expected, perpendicular OF orientation resulted in an evident resin-rich lenticular region just near the laminate surface, as visible in Figure 11(b). For the parallel orientation, there is a perfect OF embedment without causing significant perturbation in its surroundings, as shown in Figure 11(a). The presence of this lenticular region nearby the laminate interface is, probably, a main factor contributing to the detected delamination emerging in this region. It is to expect that the high distortion inflicted in the structure of the host material may contribute to the formation of cracks that will propagate in the presence of cyclic loading.

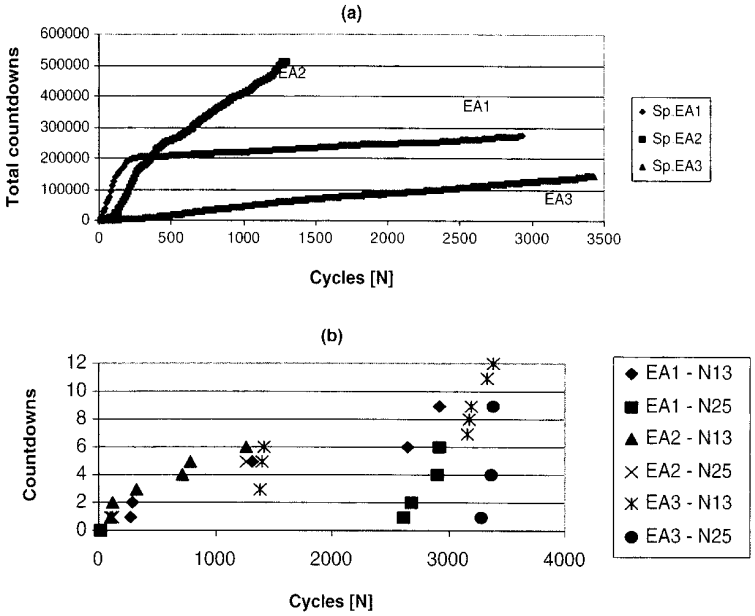

Figure 10. *Acoustic emissions for type A-M specimens: (a) total countdowns and (b) medium (N13) and high-level (N25) countdowns.*

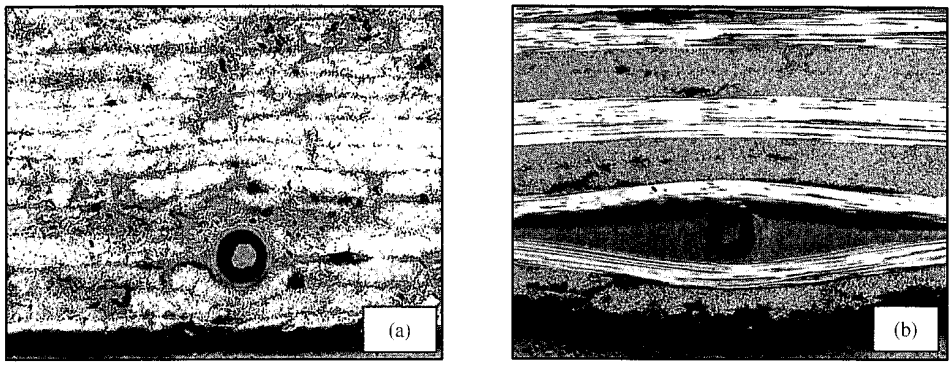

Figure 11. *Visualization of the optical fiber presence in the interior of host material: (a) parallel embedment and (b) perpendicular embedment. Magnification 50×.*

Figure 12 evidences this fact for a B-T specimen, showing an interlaminar crack with subsequent interfacial development below the abovementioned lenticular region.

Finally, other interesting evidence resulting from SEM observations was the pattern revealed at the fracture surfaces of both unidirectional and cross-ply configurations. As we can see in Figure 13, it is possible to identify two distinct regions resulting from either slow cyclic damage propagation or final breakage of specimen. In both cases shown (a) unidirectional specimen; (b) cross-ply specimen, we can distinguish the two mentioned regions, one with an airbrush-like aspect (revealing the specimen final rupture) and the other having a much more smooth texture (resulting from the slow damage propagation).

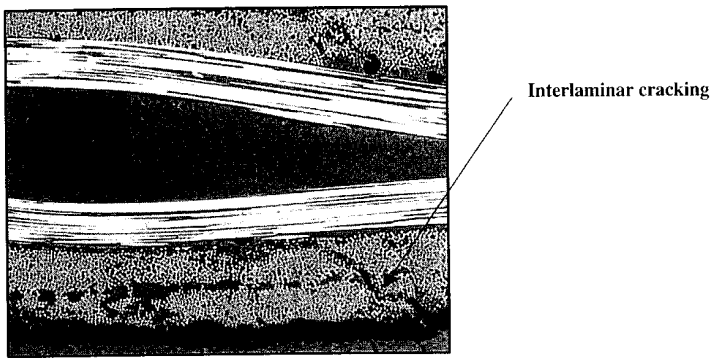

Figure 12. *Interlaminar cracking and related delamination for a B-T specimen. Magnification 100×.*

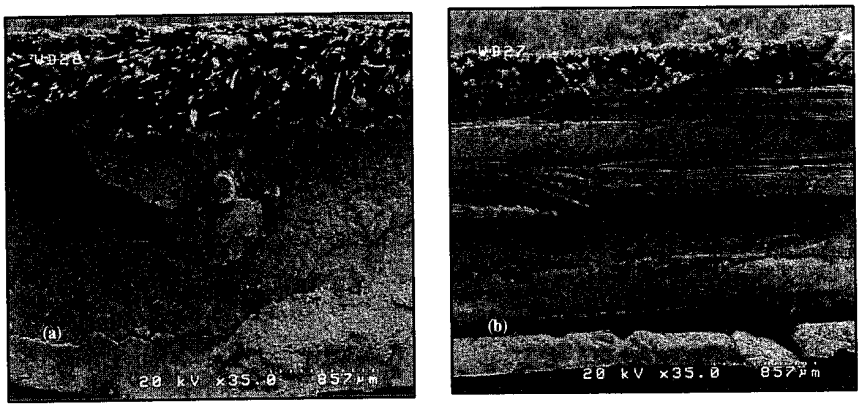

Figure 13. *Fracture surface for different configurations: (a) unidirectional specimen and (b) cross-ply specimen.*

CONCLUSIONS

The results of this investigation evince that there is actually a harmful influence on the mechanical properties of the host material resulting from embedding optical fibers. Obviously, both the nature of the effect as well as its intensity are dependent on several variables, such as loading conditions and geometrical parameters.

We can summarize the results of this research in accordance with the three different families of mechanical experiments performed as follows:

IMPACT TESTS

- The embedded optical fiber seems to act as a stress concentration agent. The phenomenon of enhanced delamination as a consequence of embedding optical fibers might be attributed to the interaction of the impact-induced stress wave with the local strain field surrounding the OF. Such interaction results in an energy release that may intensify the amplitude of the propagating stress wave.

- The extent of impact damage is dependent on the position of the optical fiber in the stacking layup. If the optical fiber is placed above the neutral zone, the effect seems to be more severe than when the optical fiber is placed below it.
- Microstructural observations have shown that delamination in low impact energy tests begins at the carbon fiber layer interface immediately below the OF.

THREE-POINT BEND TESTS

The present results confirmed the minor influence on the static mechanical properties due to the presence of OF in the host structure, when compared to similar configurations without any embedded sensor. In some cases, a small increase of strength and stiffness was even noticed but with no obvious correlation that could be attributed to the OF. Nevertheless, all variations related to strength and stiffness, resulting from confronting homologous specimen configurations, with and without OF, have never exceeded an inexpressive value of 6%.

FATIGUE TESTS

- The most critical specimen configurations contained embedded OF in the laminate middle plane. This fact was even more notorious for cross-ply laminates, which revealed premature ruptures for the higher stress ratio (90%) used in this research; for the lower loading condition (75%), a significant stiffness reduction of about 20% was detected. This behavior seems to be related to higher shear stress levels present in the middle plane.
- Some laminates with embedded OF between the third and fourth plies, for both unidirectional and cross-ply arrangements, underwent premature failure, but some others have not shown any evident damage after the conclusion of the fatigue test. Thus it can be inferred that this sensor disposition is not so detrimental as the case described above (middle plane). Surprisingly, cross-ply specimens with perpendicular embedded OF relative to adjacent plies (naturally supposed as the worst condition) did not reveal the most critical behavior, in spite of undergoing a noticeable average stiffness reduction of 12%. However, this property degradation could not be imputed exclusively to the OF presence within the material, yet some homologous configurations without sensor embedment have also evidenced some significant stiffness variation (about 25%).
- Acoustic emission tests allowed inferring quantitatively about the total level of damage development, which followed in general, a linear increasing tendency. Qualitatively, it was possible to establish that, as expected, damage occurrences start from low intensity phenomena, such as matrix cracking, following a crescent evolution and ending with higher level events, typically large delaminations and fiber breakage.
- Microstructural observations enabled to clearly identify the existence of a lenticular region surrounding the perpendicularly oriented OF relative to adjacent plies. In some cases, this highly distorted region promoted interlaminar and subsequent interfacial cracking during the fatigue tests, confirming this OF orientation as the worst case regarding the material overall mechanical behavior.

ACKNOWLEDGMENTS

The authors wish to thank the Portuguese Fundação de Ciência e Tecnologia that supported (through the Unity of R&D # 202) the present investigation. The authors are

also indebted to Engª Ana Paula de Ascenção Gomes for her personal help at the beginning of this research work and technical assistance in the SEM observations.

REFERENCES

1. Rogers, C.A. (1992). Intelligent Material Systems – The Dawn of a New Materials Age, Center for Intelligent Materials Systems and Structures, Virginia Polytechnic Institute, Blacksburg, VA.
2. Crawley, E. (1993). Intelligent Structures – A Technology Overview and Assessment, In: *Proc. 75th Meeting of the AGARD Structures and Materials*, Paper 6.
3. Lin, M. and Chang, F. (1999). Composite Structures With Built-in Diagnostics, *Materials Today*, **2**: 18–22.
4. Fuhr, P.L. (1994). Single-fiber Simultaneous Vibration Sensing and Impact Detection for Large Space Structures, *Smart Mater. Struct.*, **3**: 124–128.
5. Measures, R.M. (1989). Smart Structures with Nerves of Glass, *Prog. Aerospace Sci.*, **26**: 289–351.
6. Udd, E. (1995). *Fiber Optic Smart Structures*, John Wiley & Sons, New York, NY.
7. Foedinger, R., Rea, D., Sirkis, J., Baldwin, C., Troll, J., Grande, R., Davis, C. and VanDiver, T. (1999). Embedded Fiber Optic Sensor Arrays for Structural Health Monitoring of Filament Wound Composite Pressure Vessels, In: *Smart Structures and Materials, Proceedings of SPIE*, pp. 289–301.
8. Sirkis, J. and Dasgupta, A. (1993). The Role of Local Interaction Mechanics in Fiber Optic Smart Structures, *Journal of Intelligent Material Systems and Structures*, **4**: 260–271.
9. Carman, G. and Sendeckyj, G. (1995). Review of the Mechanics of Embedded Optical Sensors, *Journal of Composites Technology & Research*, **17**: 183–193.
10. Eaton, N., Curran, M., Dakin, J. and Geiger, H. (1993). Factors Affecting the Embedding of Optical Fiber Sensors in Advanced Composite Structures, In: *Proc. 75th Meeting of the AGARD Structures and Materials*, Paper 20.
11. Measures, R. (1993). Fiber Optic Sensing for Composite Smart Structures, In: *Proc. 75th Meeting of the AGARD Structures and Materials*, Paper 11.
12. Roberts, S. and Davidson, R. (1991). Mechanical Properties of Composite Materials Containing Embedded Fiber Optic Sensors, *Fiber Optic Smart Structures and Skins IV – SPIE*, vol. 1588, pp. 326–341.
13. Correia, H. and Devezas, T. (2000). Bending Strength of Carbon-Fibre Reinforced Composites with Embedded Optical Fibres (in Portuguese), 7ª Jornadas de Fractura – SPM: 230–237, Covilhã.
14. Surgeon, M. and Wevers, M. (1999). Static and Dynamic Testing of a Quasi-Isotropic Composite with Embedded Optical Fibers, *Composites Part A – Applied Science and Manufacturing*, 317–324.
15. Silva, J.M.A., Ferreira, J.A.M. and Devezas, T.C. (2003). Fatigue Damage of Carbon Epoxy Laminates with Embedded Optical Fibres, *Materials Science and Technology*, **19**: 809–814.
16. Jensen, D. and Koharchik, M. (1991). Cyclic Loading of Composite-Embedded Fiber-Optic Strain Sensors, In: *Proc. Spring Conf. of SEM*, pp. 233–238.
17. Jensen, D. and Brzenchek, D. (1992). Fatigue of a Composite Laminate with Embedded Optical Fibers, In: *Proc. Spring Conf. of SEM*, pp. 1319–1325.
18. Lee, D.G., Mitrovic, M., Friedman, A., Carman, G.P. and Richards, L. (2002). Characterization of Fiber Optic Sensors for Structural Health Monitoring, *Journal of Composite Materials*, **36**: 1349–1366.
19. Glossop, N.D.W., Dubois, S., Tsaw, T., Leblanc, M., Lymer, J., Measures, R.M. and Tennyson, R.C. (1990). Optical Fiber Damage Detection for an Aircraft Composite Leading Edge, *Composites*, **21**(1): 71–80.

20. Chang, C.C. (1991). Low Velocity Impact of Laminated Graphite/Epoxy Panels with Embedded Optical Fibers, MS Thesis, University of Maryland.
21. Sirkis, J.S., Chang, C.C. and Smith, B.T. Low Velocity Impact of Optical Fiber Embedded Laminated Graphite/Epoxy Panels. Part I: Macro-Scale, *J. of Composite Materials*, **28**(14): 1347–1370.
22. Poon, C., Benak, T. and Gould, R. (1990). Assessment of Impact Damage in Toughned Resin Composites, *Theoretical and Applied Fracture Mechanics*, **13**: 81–97.
23. ASTM International D790-03 (2003). Standard Test Methods for Flexural Properties of Unreinforced and Reinforced Plastics and Electrical Insulating Materials, In: *Book of Standards*, Vol. 08.01.
24. Surgeon, M. and Wevers, M. (1998). Quantifying the Damage State of Quasi-Isotropic CFRP with Embedded Optical Fibers During Fatigue Testing using Acoustic Emission and Microfocus Radiography, In: *Proc. 7th European Conference on Non-Destructive Testing*, Vol. 3, Paper 27.